

Chapter 19

Performance Comparison of Sodium and Magnesium Chloride-Saturated Solar Ponds

Ismail Bozkurt, Sibel Deniz, Mehmet Karakilcik, and Ibrahim Dincer

Abstract This chapter deals with an experimental investigation of energy efficiency of sodium and magnesium chloride-saturated solar ponds. The solar pond systems are filled with varying-density sodium and magnesium chloride water in order to form gradient layers. A solar pond generally consists of three zones. The density of the zones increases toward the bottom. Solar radiation is absorbed by salty water and the temperature rises. The high-temperature salty water at the bottom of the solar pond remains denser than less salty water above it. Thus, the convective heat losses are prevented by gradient layers. The temperature distributions of the solar pond are obtained by using thermocouples from August to November. The density of the layers was also measured and analyzed by taking samples from the same point of the temperature sensors. The efficiencies of the solar pond are defined in terms of temperatures as the average representative solar energy. As a result, the maximum energy efficiencies of the heat storage zone for the sodium and magnesium chloride-saturated solar ponds are found as 25.41 % and 27.40 % for August, respectively.

Keywords Solar energy • Solar pond • Sodium and magnesium chloride layers

I. Bozkurt

Department of Mechanical Engineering, Faculty of Engineering, University of Adiyaman, Adiyaman 02040, Turkey

S. Deniz • M. Karakilcik (✉)

Department of Physics, Faculty of Sciences and Letters, University of Cukurova, Adana 01330, Turkey
e-mail: kkilcik@cu.edu.tr

I. Dincer

Faculty of Engineering and Applied Science, University of Ontario Institute of Technology (UOIT), 2000 Simcoe Street, North Oshawa, ON, Canada L1H 7K4

Nomenclature

A	Surface area, m^2
E	Total solar energy reaching to the pond, MJ/m^2
F	Absorbed energy fraction at a region of δ -thickness
h	Solar radiation ratio
HSZ	Heat storage zone
k	Thermal conductivity, $J/m \text{ } ^\circ C$
L	Thickness of the inner zones, m
NCZ	Non-convective zone
Q	Heat, J
r	Inner radius, m
T	Temperature, $^\circ C$
UCZ	Upper convective zone

Greek Letters

η	Energy efficiency
δ	Thickness where long-wave solar energy is absorbed, m
β	Incident beam entering rate into water
θ	Angle

Subscripts

a	Ambient
i	Incident
r	Refraction
sw	Side wall

19.1 Introduction

Turkey is an energy-importing country; more than half of the energy requirement has been supplied by imports. On the other hand, Turkey has young population and growing energy demand per person [1]. The renewable energy sources should be used in Turkey to get rid of dependence on foreign energy. Solar energy is accepted as a key alternative energy source for the future. Therefore, solar energy is considered for satisfying significant part of the energy demand in Turkey [2]. Solar ponds appear to have significant potential for solar energy storage as thermal energy.

Recently, there has been increasing interest in solar pond's performance. Karakilcik et al. [3] investigated the thermal performance of an insulated salt gradient solar pond. Bozkurt and Karakilcik [4] studied heat storage performance

investigation of integrated solar pond and collector system. Karakilcik et al. [5] presented an experimental investigation of energy distribution, energy efficiency, and ratios of the energy efficiency with respect to shading effect on each zone of a small rectangular solar pond. Bozkurt et al. [6] studied the effect of the transparent covers (glass, polycarbonate, and mica) on the small cylindrical solar pond performance. Sodium chloride salt has been used in most of these studies. However, magnesium chloride salt was used in few solar ponds [e.g., 7–9].

This work deals with experimental investigation of energy efficiency of sodium and magnesium chloride-saturated solar ponds and comparison of the energy efficiencies for heat storage zones (HSZ) of the solar ponds.

19.2 System Description

An artificially constructed pond in which significant temperature rises are caused to occur in the lower regions by preventing convection is called “solar pond” [10]. Solar ponds are composed of three zones. The bottom zone of the solar pond is filled by using saturated salty water. This zone is called as HSZ and useful heat energy is stored in here. The middle zone of the pond is non-convective zone (NCZ). NCZ is composed of salty water layers whose brine density gradually increases toward the surface of the solar pond. The density gradient in NCZ is very important to keep the stored energy in HSZ. The surface zone of the pond is upper convective zone (UCZ). UCZ is the freshwater layer at the top of the pond. This zone is fed with freshwater in order to maintain its density close to the density of freshwater and to replenish the lost water due to evaporation [4].

In this study, we constructed sodium and magnesium chloride-saturated solar ponds to determine the energy efficiency. Figure 19.1 shows a schematic representation of the solar pond.

The solar ponds have a radius of 0.48 m and a depth of 1.10 m; the bottom and the side walls of the pond were plated with the PVC sheets in 5 mm thickness, and in between with a glass wool of 10 cm thickness as outer surface insulating layer. The solar pond’s inner zones possess different density levels of salty water. Salty waters with different density are prepared in the plastic tanks in order to form the solar pond. The thicknesses of the UCZ, NCZ, and HSZ are 0.1 m, 0.50 m, and 0.50 m, respectively. The range of salt gradient in the inner zones is such that the densities are 1,000–1,020 kg/m³ in UCZ, 1,020–1,160 kg/m³ in NCZ, and 1,150–1,180 kg/m³ in HSZ.

19.3 Energy Analysis

The temperature distributions in the solar pond and the incident radiation reaching on the surface of the pond were determined, experimentally. To calculate the heat storage efficiency of the solar pond, the energy balance equations were written.

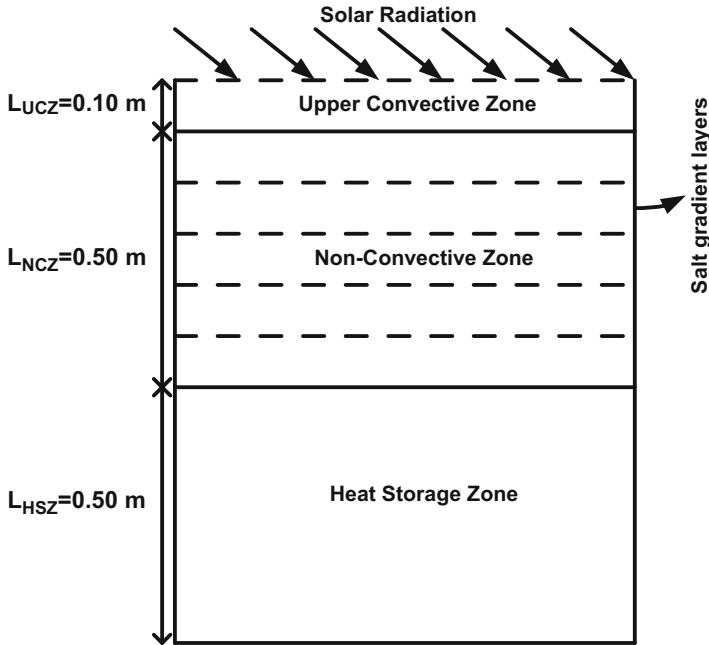


Fig. 19.1 Schematic representation of the solar pond

In this study, we focus on the heat fluxes in HSZ because the useful heat energy is stored in HSZ. The energy balance equation of HSZ is written as follows:

$$Q_{\text{stored}} = Q_{\text{solar,HSZ}} - Q_{\text{loss,HSZ}} \tag{19.1}$$

where Q_{stored} is stored heat energy in the HSZ of the solar pond, $Q_{\text{solar,HSZ}}$ is the amount of net solar energy which is absorbed in the zone, and $Q_{\text{loss,HSZ}}$ is the heat loss from the HSZ to outside of the pond.

$Q_{\text{solar,HSZ}}$ is defined as

$$Q_{\text{solar,HSZ}} = \beta EA_{\text{HSZ}}[(1 - F)h(x - \delta)] \tag{19.2}$$

where E is the total solar energy reaching the solar pond surface, A_{HSZ} is the area of the HSZ which is subjected to solar insolation, F is the fraction of energy absorbed at a region of δ -thickness, h is the solar radiation ratio, and x is the thickness of the UCZ. β is the fraction of the incident solar radiation that actually enters the pond and is given by Hawlader [11] as follows:

$$\beta = 1 - 0.6 \left[\frac{\sin \theta_i - \sin \theta_r}{\sin \theta_i + \sin \theta_r} \right]^2 - 0.4 \left[\frac{\tan \theta_i - \tan \theta_r}{\tan \theta_i + \tan \theta_r} \right]^2 \tag{19.3}$$

Here, θ_i and θ_r are the incidence and refraction angles. h represents the ratio of the solar energy reaching the depth in the layer I to the total solar incident falling on to the surface of the pond and is given by Bryant and Colbeck [12] as

$$h = 0.727 - 0.056 \ln \left[\frac{(x_1 - \delta)}{\cos \theta_r} \right] \quad (19.4)$$

where x_1 is the thickness of the layer, and δ thickness of the layer in the UCZ where long-wave solar energy is absorbed. $Q_{\text{loss,HSZ}}$ is defined as

$$\begin{aligned} Q_{\text{loss,HSZ}} &= Q_{\text{up}} + Q_{\text{side}} + Q_{\text{down}} \\ &= \frac{k_s A}{\Delta x_{\text{HSZ-NCZ}}} (T_{\text{HSZ}} - T_{\text{NCZ}}) + \frac{k_{\text{sw}} 2\pi r L_{\text{HSZ}}}{\Delta x_{\text{side}}} (T_{\text{HSZ}} - T_a) + \frac{k_{\text{sw}} A}{\Delta x_{\text{down}}} (T_{\text{down}} - T_a) \end{aligned} \quad (19.5)$$

where Q_{down} is the total heat loss to the down wall from HSZ, and Q_{up} is the heat loss from HSZ to the above zone. Q_{side} is the total heat loss to the side walls of the solar pond. A is the surface area of the solar pond, T_a is the ambient air temperature, k_{sw} is the thermal conductivity of the side and bottom walls, k_s is the thermal conductivity of the salty water, L_{HSZ} is the thickness of the HSZ (m), r is the inner radius of the cylindrical solar pond, Δx_{down} is the thickness of the down wall, Δx_{side} is the thickness of the side wall, and $\Delta x_{\text{HSZ-NCZ}}$ is the thickness of the HSZ's middle point and the NCZ's middle point. The energy efficiency of the solar pond can be defined as follows:

Substituting Eq. (19.5) in Eq. 19.1 for the HSZ yields the following expression for the energy efficiencies:

$$\eta = \frac{Q_{\text{stored}}}{Q_{\text{solar,HSZ}}} = 1 - \frac{\{Q_{\text{down}} + Q_{\text{up}} + Q_{\text{side}}\}}{Q_{\text{solar,HSZ}}} \quad (19.6)$$

Substituting equations for each parameter in Eq. 19.6 provides us with the following energy efficiency:

$$\eta_{\text{HSZ}} = 1 - \frac{\left\{ \frac{k_s A}{\Delta x_{\text{HSZ-NCZ}}} (T_{\text{HSZ}} - T_{\text{NCZ}}) + \frac{k_{\text{sw}} 2\pi r L_{\text{HSZ}}}{\Delta x_{\text{side}}} (T_{\text{HSZ}} - T_a) + \frac{k_{\text{sw}} A}{\Delta x_{\text{down}}} (T_{\text{down}} - T_a) \right\}}{\beta E A_{\text{HSZ}} [(1 - F)h(x - \delta)]} \quad (19.7)$$

19.4 Results and Discussion

In this work, we present the results of the energy efficiency for both sodium and magnesium chloride-saturated solar ponds. The stability of salt density distribution has a great significance to protect convection heat losses from the HSZ of the solar pond. Figure 19.2 shows the density distribution of the sodium and magnesium chloride solar pond. As seen in Fig. 19.2, there are little differences between these

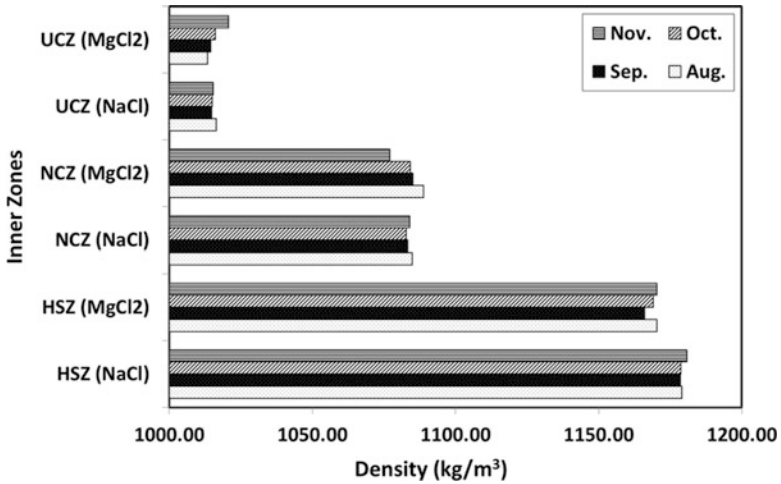


Fig. 19.2 The density distributions of the sodium and magnesium chloride solar ponds

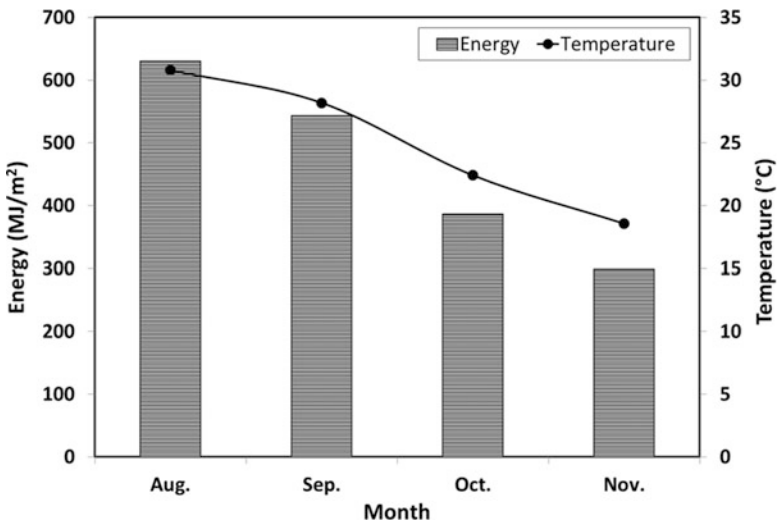


Fig. 19.3 The variations of the solar energy and air temperature distributions

density distributions. The density distributions are kept approximately stable by using the salt gradient protection system in order to inject high-density saline water at the top layer of the HSZ. Figure 19.3 shows the variations of the solar energy and air temperature in Adana, Turkey.

As seen in Fig. 19.3, the maximum and minimum solar energy are 630.00 MJ/m² in August and 298.12 MJ/m² in November during 4 months, and the maximum and minimum average air temperature are 30.80 °C in August and 18.56 °C in November during 4 months.

Sodium and magnesium chloride-saturated solar ponds were used to store the heat energy. The experimental temperature measurements were taken from the solar ponds on an hourly basis. Figure 19.4 shows average experimental temperature distributions measured inside the solar ponds during 4 months. As shown in Fig. 19.4 the maximum average temperatures of HSZ are 41.87 °C and 52.42 °C in August for sodium and magnesium chloride-saturated solar ponds, respectively. Figures 19.5 and 19.6 show the variation of the energy input, stored, and losses from August to November for sodium and magnesium chloride-saturated solar ponds.

The energy distributions were calculated by using temperature distributions of the solar pond and the reference air temperature. As seen in Figs. 19.5 and 19.6, the

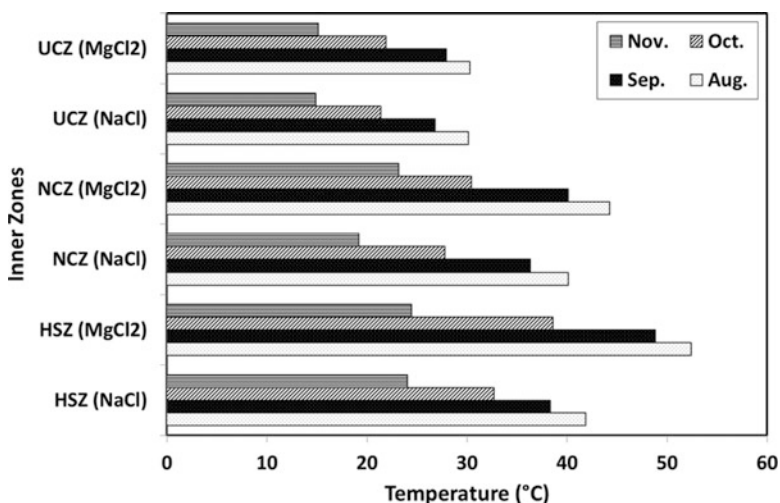


Fig. 19.4 The average experimental temperature distributions of the inner zones

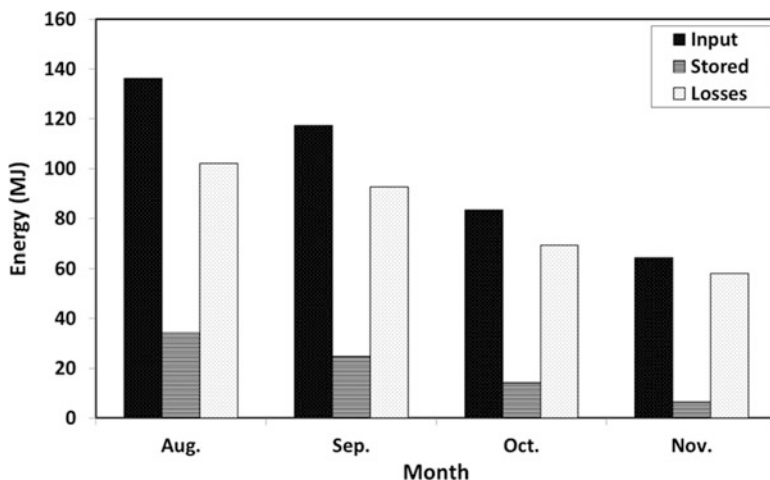


Fig. 19.5 Variations of the energy input, stored, and losses for sodium chloride-saturated pond

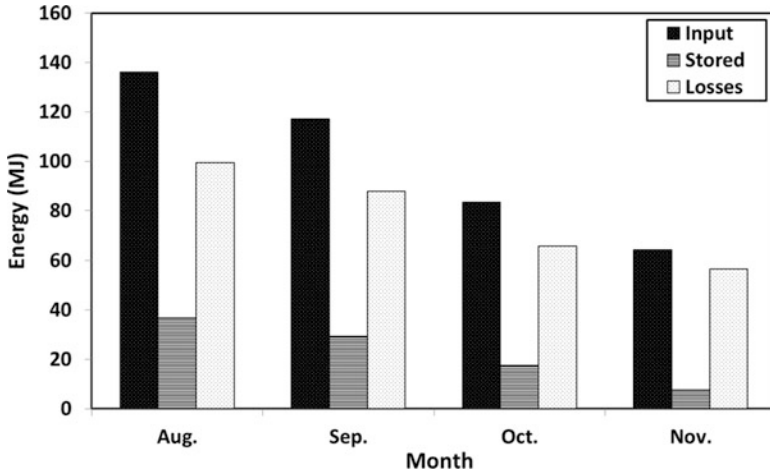


Fig. 19.6 Variations of the energy input, stored, and losses for magnesium chloride-saturated ponds

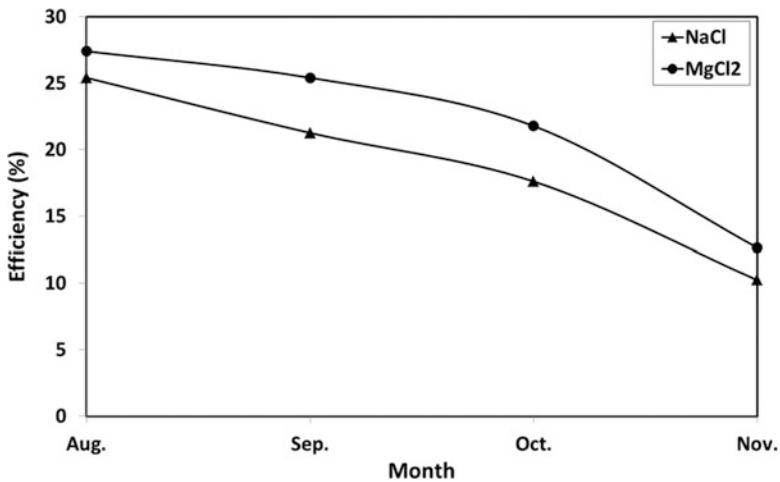


Fig. 19.7 The efficiencies of the sodium and magnesium chloride-saturated ponds

energy stored appears to be maximum at 34.02 MJ and 36.74 MJ in August and minimum at 6.44 MJ and 7.73 MJ in November for sodium and magnesium chloride-saturated solar ponds, respectively.

The efficiencies are dependent on the heat losses, and the temperatures of the salty water and air. The energy losses in the zones were calculated. The energy efficiencies were determined for the solar ponds during the months August, September, October, and November. Figure 19.7 shows the efficiencies of the sodium and magnesium chloride-saturated ponds.

As seen in Fig. 19.7, the maximum and minimum efficiencies of the solar pond were seen to occur in August and November. The highest efficiencies were observed to be 25.41 % and 27.40 % for sodium and magnesium chloride-saturated solar ponds, respectively.

19.5 Conclusion

In this chapter, we have studied both sodium and magnesium chloride-saturated solar ponds' performances. The energy efficiencies are determined for the HSZ of the solar ponds by using the experimental data. The efficiencies are dependent on the heat losses, temperatures of the inner zones and ambient air, incoming solar radiation, and turbidity of the salty water. By comparison, magnesium chloride-saturated solar pond stores more heat energy than sodium chloride-saturated solar pond.

Acknowledgements The authors are thankful to University of Cukurova for financial support of this work (Grant No. FEF2010BAP5 and FEF2012YL13).

References

1. Canyurt OE, Ozturk HK (2008) Application of genetic algorithm (GA) technique on demand estimation of fossil fuels in Turkey. *Energ Pol* 36:2562–2569
2. Bulut H, Buyukalaca O (2007) Simple model for the generation of daily global solar-radiation data in Turkey. *Appl Energ* 84:477–491
3. Karakilcik M, Kıymaç K, Dincer I (2006) Experimental and theoretical distributions in a solar pond. *Int J Heat Mass Transfer* 49:825–835
4. Bozkurt I, Karakilcik M (2012) The daily performance of a solar pond integrated with solar collectors. *Sol Energ* 86:1611–1620
5. Karakilcik M, Dincer I, Bozkurt I, Atiz A (2013) Performance assessment of a solar pond with and without shading effect. *Energ Convers Manag* 65:98–107
6. Bozkurt I, Atiz A, Karakilcik M, Dincer I (2014) Transparent covers effect on the performance of a cylindrical solar pond. *Int J Green Energ* 11:404–416
7. Subhakar D, Murthy SS (1991) Experiments on a magnesium chloride saturated solar pond. *Renew Energ* 5–6:655–660
8. Subhakar D, Murthy SS (1993) Saturated solar ponds: 2. Parametric studies. *Sol Energ* 50:307–319
9. Subhakar D, Murthy SS (1994) Saturated solar ponds: 3. Experimental verification. *Sol Energ* 53:469–472
10. Ranjan KR, Kaushik SC (2014) Thermodynamic and economic feasibility of solar ponds for various thermal applications: a comprehensive review. *Renew Sustain Energ Rev* 32:123–139
11. Hawlader MNA (1980) The influence of the extinction coefficient on the effectiveness of solar ponds. *Sol Energ* 25:461–464
12. Bryant HC, Colbeck I (1977) A solar pond for London. *Sol Energ* 19:321–322